An Adaptive Snow Identification Algorithm in the Forests of Northeast China

Xiaoyan Wang, Siyong Chen, and Jian Wang

***Abstract*—Northeast China is one of the primary snow-covered regions, and its forest coverage is over 40%. Forest snow identification is usually a challenging problem, and the SNOMAP algorithm tends to underestimate the amount of snow cover in forest regions for the lower normalized difference snow index. In this article, an improved method of the snow-cover identification based on the Landsat operational land imager is proposed. One improvement includes using the normalized difference forest snow index (NDFSI) to discriminate between snow-covered and snow-free forests. The threshold value of the NDFSI in different forest types is set according to the normalized difference vegetation index. On the other hand, the sun elevation is very low in winter in Northeast China with high latitude; as a result, the snow in shadow areas is usually classified as liquid water for its low near-infrared reflectance in the current SNOMAP algorithm. Then, another improvement is introducing the land surface temperature, which is retrieved from the thermal infrared band to distinguish liquid water from snow in shadow areas. We applied this improved method to evaluate forest areas in the Daxinganling, Xiaoxinganling, and Changbai Mountain areas in different seasons. The total classification accuracy reached 97.5%, and the pixels that introduce omission error and commission error were mainly distributed in areas of dense forest shadows. This improved method retains the computational simplicity and effectiveness of the SNOMAP algorithm in nonforest areas and improves the underestimation of snow cover in forest regions and shadow areas.**

***Index Terms*—Forest, normalized difference snow index (NDSI), Northeast China, remote sensing, snow cover.**

I. Introduction

SNOW cover is a critical component of the cryosphere and climate system, and it plays an important role in the global energy balance and atmospheric circulation due to its high albedo and low thermal conductivity [1], [2]. It is necessary to accurately assess seasonal snow cover for understanding the present and future climate, water cycle, and ecological changes [3]–[11]. At present, several snow-cover area estimation algorithms based on remote sensing have been developed, such as spectral mixture analysis [12]–[15], linear models of snow-cover reflectance [16]–[18], and artificial neural networks [19], [20]. Although a broad variety of remotely sensed datasets and advanced snow-cover monitoring methods are available, the spatial and temporal distributions of snow cover in forest regions remain poorly understood [21]–[24].

SNOMAP is a popular binary snow/nonsnow mapping algorithm for thematic mapper (TM), operation land imager (OLI), advanced very high-resolution radiometer (AVHRR), and moderate resolution imaging spectroradiometer (MODIS) images, in which the normalized difference snow index (NDSI) plays a key role in detecting snow cover [25]–[27]. The high reflectance in the visible spectrum compared with that in the midinfrared portion of the spectrum yields high NDSI values for snow compared with other surface materials. For snow in forest areas, sensors receive a mixed spectrum from snow and the forest crown. Therefore, the NDSI, which was proposed based on the spectral characteristics of snow in open areas, will not effectively distinguish snow-covered forests from snow-free forests [17].

Some studies have focused on snow-cover mapping in forest areas, but the accuracy of the results requires further verification. Klein *et al*. [28] proposed an additional criteria test that incorporated NDSI and normalized difference vegetation index (NDVI) values to classify snow-covered forest pixels. However, the field boundaries of NDSI-NDVI values are not very clear in Northeast China due to the complexity of the forest. Adjusting the NDSI threshold downward would permit more snow in forests to be mapped as snow, but in doing so, nonsnow pixels may also be mapped as snow. A snow-cover mapping method for forests, which is called SnowFrac, is a linear spectral hybrid model based on snow cover, trees, and snow-free ground to estimate the snow-cover area in forest regions [29], [30]. The operation of this model requires high-precision forest cover maps as prior knowledge. In the model of mapping the fraction of snow-covered area in the boreal zone (SCAmod), the fraction of snow cover (FSC) is a function of the satellite observation reflectance of a single band, and the test results for all watersheds in Finland with NOAA/AVHRR data showed that the model can effectively estimate FSC in forest areas [31]. Czyzowska-Wisniewski *et al*. [32] developed the Landsat TM FSC estimation method based on an artificial neural network (ANN); the network uses up to 15 input parameters, such as the reflectance of six bands, slope, aspect, and shade. The accuracy of this algorithm is high in a small region, but it is not suitable for snow identification in large-area forests due to its complexity.

Manuscript received May 26, 2020; revised July 24, 2020 and August 17, 2020; accepted August 18, 2020. Date of publication August 28, 2020; date of current version September 11, 2020. This work was supported in part by the National Natural Science Foundation of China under Grant 41771373 and in part by the Science and Technology Basic Resources Investigation Program of China under Grant 2017FY100500. *(Corresponding author: Xiaoyan Wang.)*

Xiaoyan Wang and Siyong Chen are with the College of Earth and Environmental Sciences, Lanzhou University, Lanzhou 730000, China (e-mail: wangxiaoy@lzu.edu.cn; chensy18@lzu.edu.cn).

Jian Wang is with the Northwest Institute of Eco-Environment and Resources, Chinese Academy of Sciences, Lanzhou 730000, China (e-mail: wjian@lzb.ac.cn).

Digital Object Identifier 10.1109/JSTARS.2020.3020168

According to the spectral difference between snow-covered and snow-free forest areas, an index named the normalized difference forest snow index (NDFSI), defined as $\mathrm{NDFSI} = (\rho_{\mathrm{nir}} - \rho_{\mathrm{swir}})/(\rho_{\mathrm{nir}} + \rho_{\mathrm{swir}})$, was proposed for snow identification in the upper Heihe River basin (UHRB) [33]. Combined with a classification map, the overall accuracy of snow mapping in forest regions can reach 93.92% with this method. A snow mapping algorithm based on a combined multi-index technique that combines the NDSI, NDFSI, and NDVI was developed and applied to the mountainous forested areas of northern Xinjiang, China [34]. In that application, the NDVI was added to prevent dense vegetation with high NDFSI values from being classified incorrectly as snow in forest areas. In forest regions, the total accuracy of snow-cover mapping during the snowmelt period was 93.2%. During the full snow-covered period, the method based on the multi-index technique detected 94.5% of the snow in forest regions. The dominant forest type in these two study areas is evergreen coniferous forests.

Northeast China is one of the primary snow-covered regions in China, and the forest coverage is over 40% [35]. The forests are mainly distributed in the Daxinganling, Xiaoxinganling, and Changbai Mountain areas. The forest types include evergreen coniferous forests and deciduous forests. Understanding the distribution and the melting trends of forest snow cover can provide guidance for agriculture and forest management in Northeast China. Landsat data at a resolution of 30 m are usually used to validate MODIS snow products [36]–[39]; however, the Landsat snow mapping results based on the SNOMAP algorithm are unreliable in forest regions. In this study, we selected typical forest areas from the Landsat OLI images of Northeast China, analyzed the spectral characteristics of these areas and the distribution of reflectivity index values for different forest types in different seasons, and developed a high-accuracy snow identification algorithm suitable for the forest areas of Northeast China. This algorithm adds some rules to identify snow in forest areas without detracting from the simplicity and effectiveness of the SNOMAP algorithm in nonforest areas.

The rest of this article is organized as follows. Section II describes the study area and the datasets used in this article. Section III presents the methodology, and the experimental results are given in Section IV. Finally, Section V concludes this article.

II. Study Area and Data

The study area is located in Northeast China, and the sites represent a seasonally snow-covered boreal forest. In this area, snow is usually from the end of November to the middle of March and the snow cover is rather homogenous. The forest coverage is over 40% in the study area, and Daxinganling, Xiaoxinganling, and Changbai Mountains are the main forest cover areas. Daxinganling is in the northern part of Northeast China, which has a cold climate. The dominant forest types in Daxinganling are deciduous species such as larch and birch. Xiaoxinganling and Changbai Mountains are located in warmer areas than Daxinganling, and the forest types are mainly temperate coniferous and broad-leaved mixed forests. The dominant forests in Xiaoxinganling and Changbai Mountains are evergreen species such as Korean pine, spruce, and fir, and there are some deciduous broad-leaved forests with Mongolian oak and birch [40]. Rich snow cover and forest diversity make Northeast China an ideal region for forest snow research. The study area is shown in Fig. 1.

The OLI images used in this study and descriptions of the real scenes are listed in Table I. These images were acquired under clear sky conditions in different seasons, including at fully snow-covered, partially snow-covered, and snow-free times. Images 1–3 are of the Daxinganling area (L1 in Fig. 1). Images 4–6 are of the Xiaoxinganling area (L2 in Fig. 1). Image 7 (L3 in Fig. 1) and Image 8 (L4 in Fig. 1) are of the Changbai Mountain areas. A GaoFen-1B Panchromatic Multispectral Sensor (GF-1B PMS) image with a 2-m spatial resolution, which was acquired on December 22, 2018, is used to verify the accuracy of the snow identification results for the Image 7. High spatial resolution Google Earth image was acquired on January 31, 2019, and it will provide more detailed evaluation of snow identification results for the Image 8.

III. Spectral Characteristics of the Forests in Northeast China

The regions of interest (ROIs) ROI1 and ROI2 are chosen to analyze the spectral characteristics of forest areas with and without snow. The locations of ROI1 and ROI2 are shown in Fig. 1. ROI1 encompasses 40090 pixels and is located in the Daxinganling area. The typical forest type in ROI1 is the deciduous conifer forest. ROI2 includes 49 284 pixels and is located in the Xiaoxinganling area. The typical forest type in ROI2 is evergreen coniferous forest. Fig. 2 shows the typical snow-covered forest landscapes of ROI1 and ROI2.

A. Reflection Characteristics of Forests With and Without Snow

Fig. 3 shows the reflection spectrum curves of different forests with and without snow. The red lines are drawn based on ROI1 in the Image 3 (fully snow covered) and Image 1 (without snow). The blue lines are drawn based on ROI2 in the Image 6 (fully snow covered) and Image 4 (without snow). Fig. 3 shows the following trends.

1) In winter, if it is snow-free, deciduous forests exhibit spectral characteristics that are more like soil than vegetation, and evergreen coniferous forests exhibit obvious spectral characteristics of vegetation. Additionally, the visible band reflectance of deciduous forests is higher than that of evergreen coniferous forests.
2) When a forest is covered with snow, the reflectance in the visible and near-infrared (NIR) bands will increased, including for both evergreen and deciduous forests. Moreover, the shortwave infrared (SWIR) reflectance will decrease because of the high reflectance of snow in the visible/NIR bands and the high absorption in the SWIR band.
3) Deciduous forests have higher transmittance than evergreen coniferous forests, and the reflectance in visible

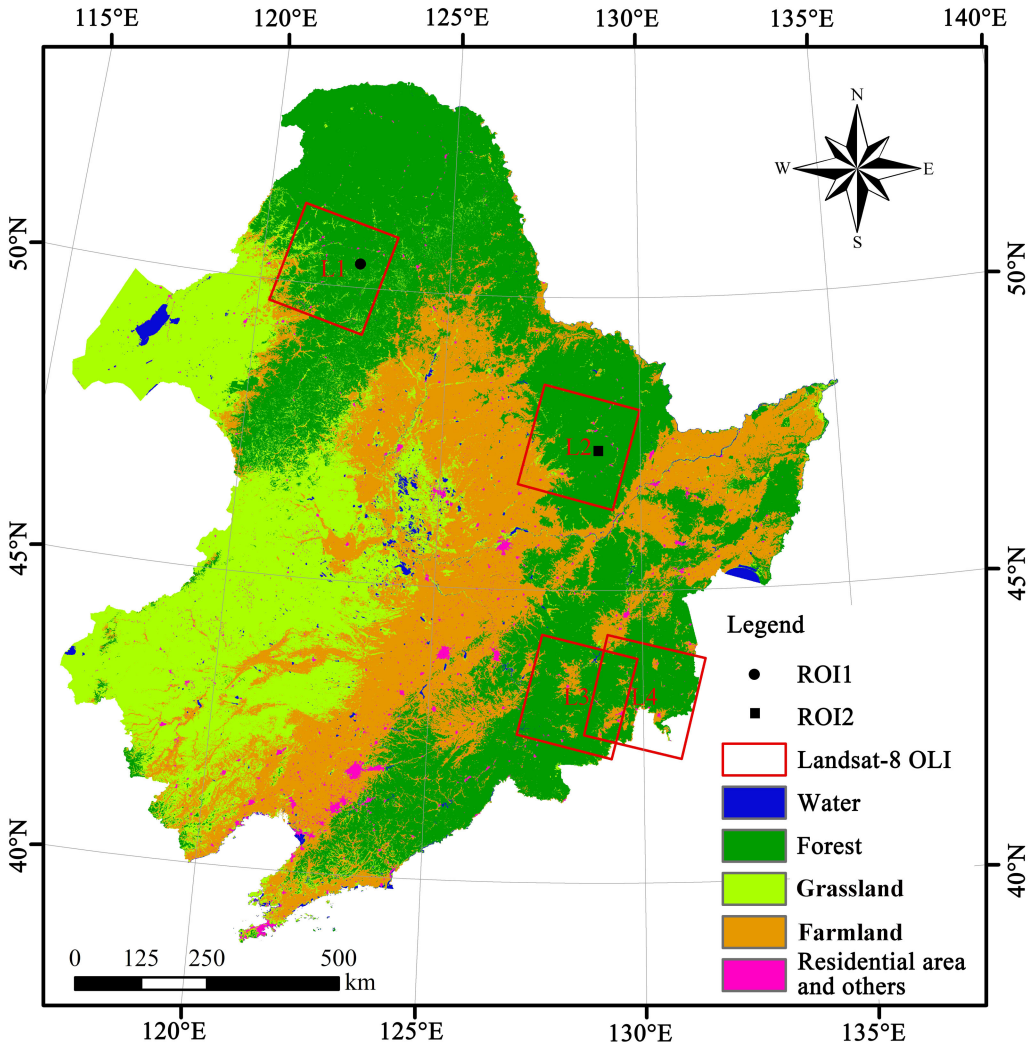

Fig. 1. Land cover map of Northeast China and OLI images used in the experiments.

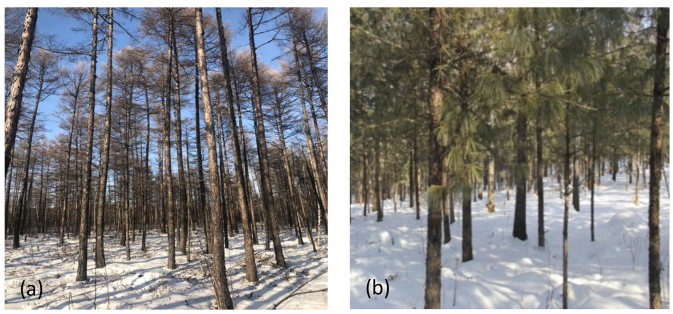

Fig. 2. Typical snow-covered forest landscapes of (a) ROI1, acquired on December 30, 2018, and (b) ROI2, acquired on January 10, 2018.

bands is higher for deciduous forests than for evergreen forests, whether the area is snow free or snow covered.

4) An interesting finding is that the reflectance in the NIR band is the same in these two forest types both with snow and without snow.

B. Reflection Indexes of Forests With and Without Snow

In open areas, the NDSI was built to discriminate between snow and other surface cover and between snow and clouds. However, it does not discriminate between snow-covered and snow-free forest areas. The NDFSI, defined as $(\rho_{\mathrm{nir}} - \rho_{\mathrm{swir}})/(\rho_{\mathrm{nir}} + \rho_{\mathrm{swir}})$, can capture the increase in NIR reflectance and decrease in SWIR reflectance and was successfully used as a snow detector for the Qinghai spruce forest area of the UHRB [33] and the Siberian spruce forest area in northern Xinjiang, China [34]. These two forests are both evergreen coniferous forests.

Northeast China includes abundant forest resources, including deciduous forests, evergreen coniferous forests, and mixed forests. Fig. 4(a) and (b) shows the NDFSI histograms of ROI1 and ROI2 with and without snow. Whether the forest is a deciduous forest or an evergreen coniferous forest, the distribution of NDFSI values obviously differs between forest with and without snow. Therefore, it is possible to distinguish snow-covered and snow-free forest areas by setting an appropriate NDFSI threshold value.

TABLE I
LANDSAT OLI IMAGES USED IN THE SNOW IDENTIFICATION EXPERIMENTS

Image	Path/row	Date (year/ month/day)	Snow coverage
1		2017/09/21	no snow cover
2	122/025 (L1 in Fig. 1)	2017/10/23	partially snow covered
3		2018/12/29	fully snow covered
4		2018/10/07	no snow cover
5	117/027 (L2 in Fig. 1)	2018/03/29	partially snow covered
6		2018/01/24	fully snow covered
7	116/030 (L3 in Fig. 1)	2018/12/19	partially snow covered
8	115/030 (L4 in Fig. 1)	2019/01/29	partially snow covered
GF-1B		2018/12/22	partially snow covered，used to evaluate the snow identification result of Image 7
Google earth		2019/01/31	partially snow covered, used to evaluate the snow identification result of Image 8

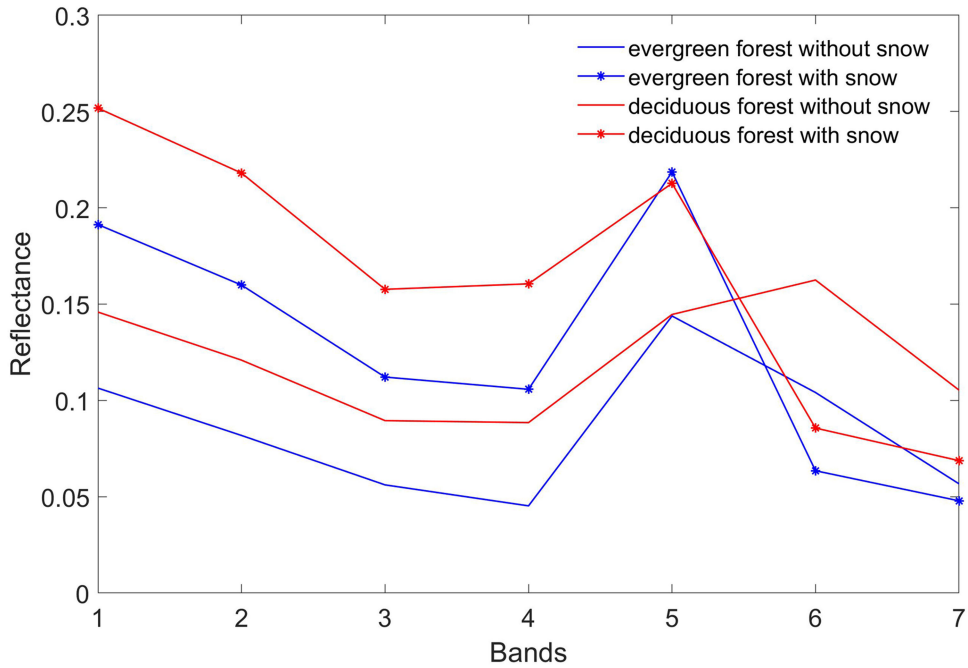

Fig. 3. Forests reflectance of ROI1 and ROI2 in OLI images with and without snow.

However, the NDFSI threshold values are different for these two forest types. In evergreen coniferous forests, the NDFSI threshold value is 0.4, as shown in Fig. 4(a), which is consistent with the value used in previous studies of the Qinghai spruce forest in the UHRB [33] and Siberian spruce forest in northern Xinjiang, China [34]. In deciduous forest areas, the NDFSI threshold value is 0.2, as shown in Fig. 4(b). Therefore, setting the NDFSI threshold value to distinguish snow in forests is challenging when accurate land cover map is not available to provide auxiliary data.

Fig. 4(c) shows that when forests are covered with snow, the NDVI value in evergreen coniferous forests ($>$0.3) is higher than

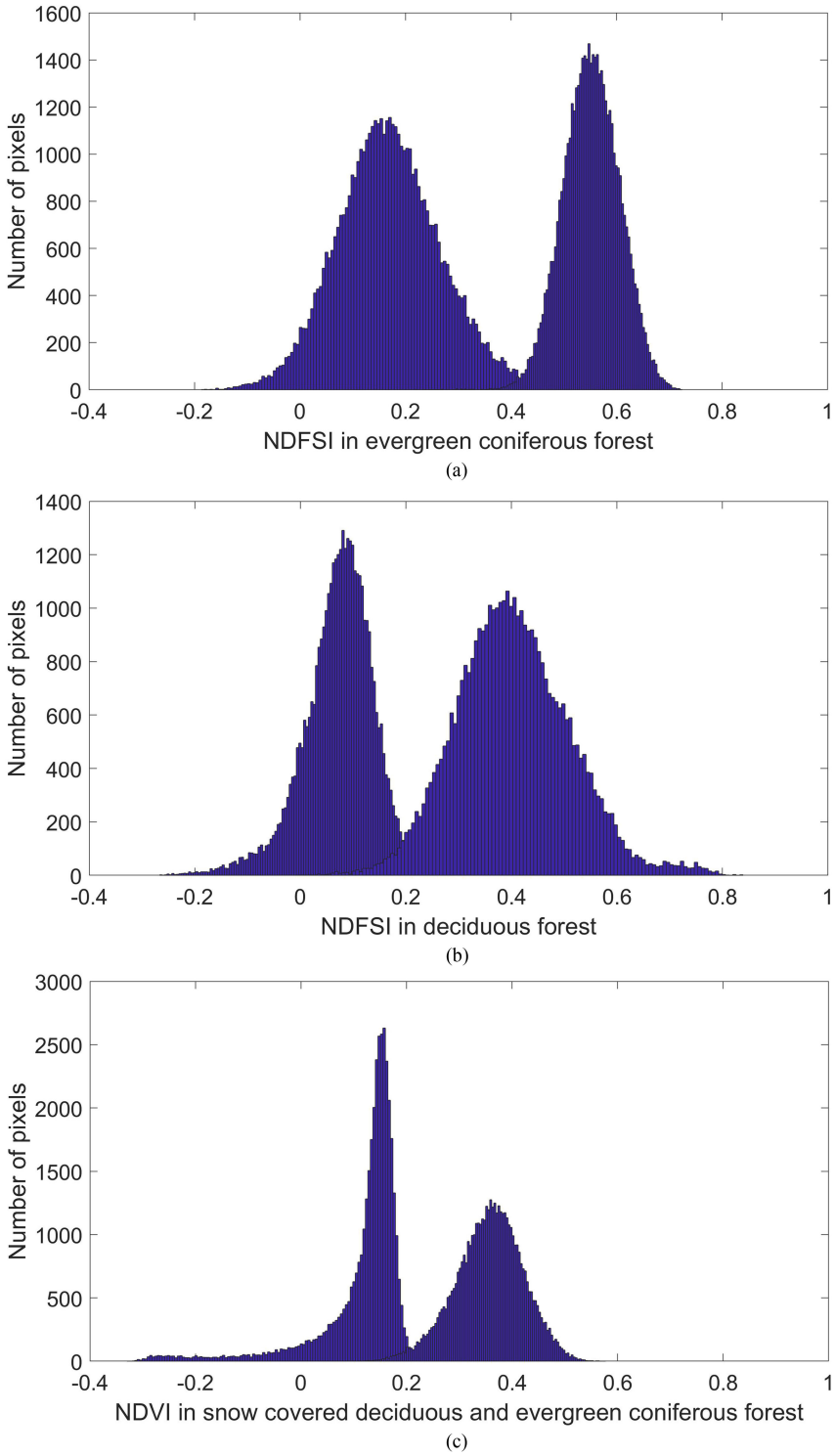

Fig. 4. Distributions of the NDFSI and NDVI in forests with snow and without snow.

that in deciduous larch forests (<0.2). Therefore, it is feasible to set the NDFSI threshold value according to the NDVI.

C. Methodology of Snow Identification in Forest Areas

As noted in Section III-B, the NDFSI is an effective index for detecting snow in both deciduous and evergreen coniferous forests, and the NDFSI threshold value is different in these two forest types and can be set based on the NDVI. Thus, an improved snow identification method is proposed for Northeast China, which has high forest coverage. This method is based on the SNOMAP algorithm, and some improvements have been made for forest regions and shade areas. The flowchart of the algorithm is shown in Fig. 5.

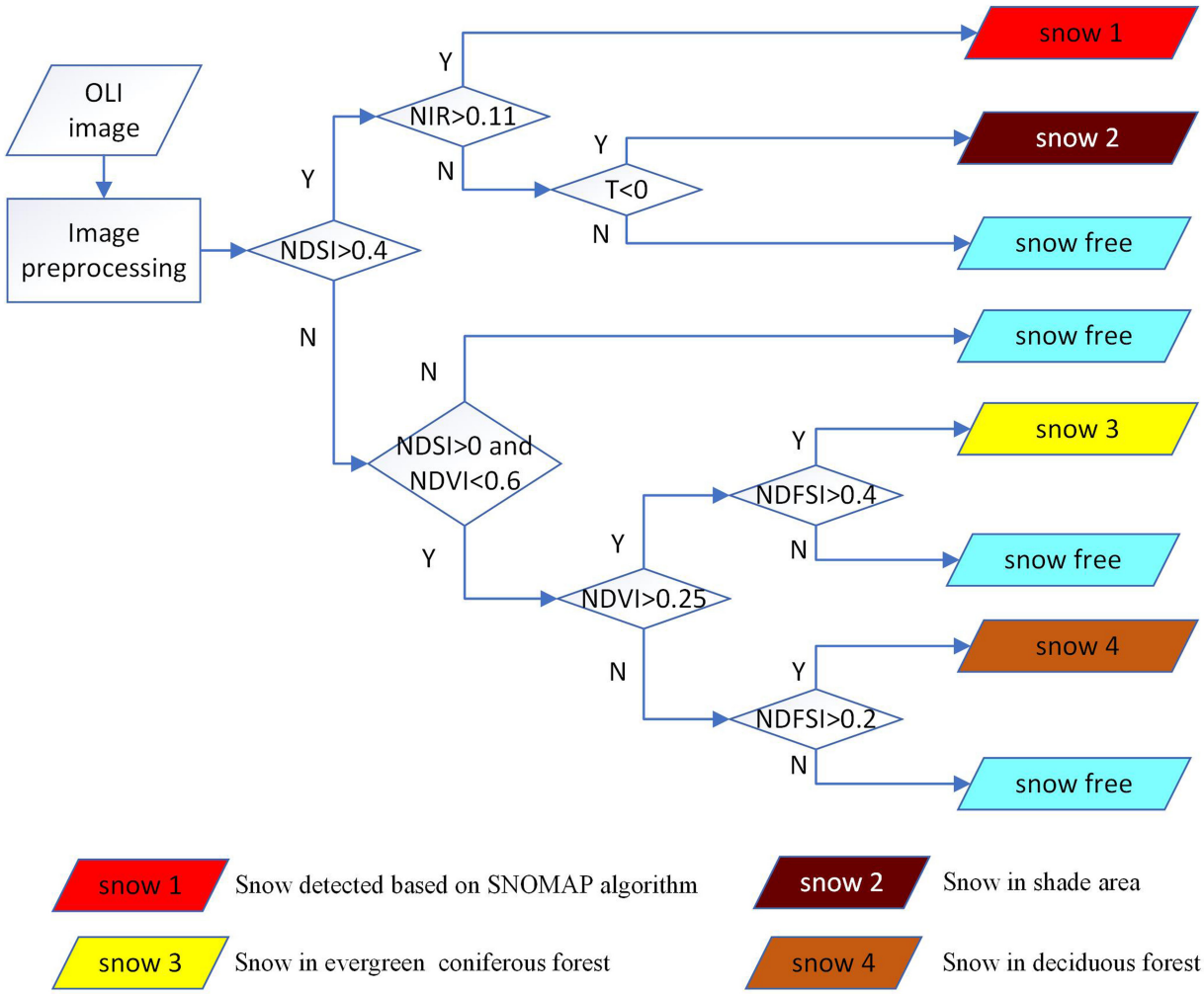

Fig. 5. Flow chart of the snow identification algorithm.

1) According to SNOMAP, the NDSI threshold is set to 0.4, with NIR>0.11. The NIR threshold is set to exclude liquid water that may also have high NDSI values. In forest regions at high latitudes, the large solar zenith angle creates shadows in winter. Snow in forest shadow areas usually has a high NDSI value, but the NIR reflectance may be low so that it is recognized mistakenly as liquid water. In the improved algorithm, a temperature mask is added. For pixels with NDSI>0.4, if T<0 °C, they will be classified as snow even if with NIR<0.11, that is snow 2 in Fig. 5. Here, T is the temperature, which is retrieved from the thermal infrared band of the OLI.
2) Pixels with NDSI<0.4 must be further evaluated to determine whether they are snow in forest areas. Here, the NDFSI index is used for further evaluation. Wang *et al.* noted that dense vegetation in summer is usually with a high NDVI and a high NDFSI [34], so the pixels with NDVI >0.6 are recognized as snow free. Whether an open area or a forest area, the NDSI is always greater than 0 when an area is covered with snow. Therefore, only the pixels with NDSI>0 and NDVI<0.6 are included in the identification process.
3) According to Fig. 4(c), the threshold value of the NDVI is set to be 0.25. For pixels with NDVI values greater than 0.25, the threshold of the NDFSI is set to 0.4 to determine if there is snow in evergreen coniferous forest areas. When the NDVI value is less than 0.25, the NDFSI is set to 0.2 to distinguish snow-covered deciduous forest from snow-free forest.

IV. Results

To acquirethe actual snow cover extent for the entire area is not possible, either through fieldobservations or aerial photography, so two simplifying assumptions are made. In Daxinganling and Xiaoxinganling area, the snow cover is assumed to be 100% in the winter scenes (Images 3 and 6) and 0% for the early autumn scenes (Images 1 and 4). These assumptions are consistent with the local meteorological data and were visually confirmed. With these two assumptions, a quantitative evaluation of the accuracy

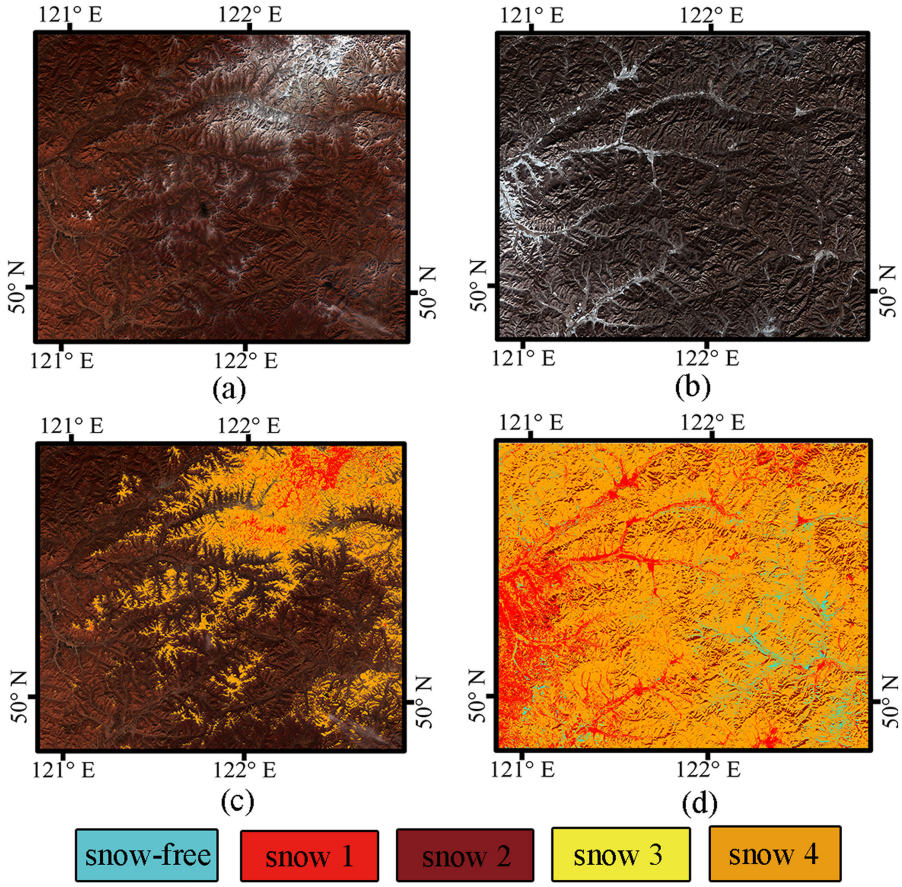

Fig. 6. OLI Images (combined with the NIR, red, and green bands) and snow identification results. (a) OLI Image 2, acquired on October 23, 2017. (b) OLI Image 3, acquired on December 29, 2018. (c) Snow identification result of Image 2. (d) Snow identification result of the Image 3.

of the modified snow-cover mapping algorithm is possible. The experiment was performed based on images with partial snow cover (Images 2 and 5), and the validation of the results was based on visual interpretation. The snow identification results for the Image 7 were validated with a GF-1B PMS image (with 2-m spatial resolution) that was acquired at nearly the same time as the Image 7. Google Earth Image with very high spatial resolution will give more detailed evaluation of snow identification results for the Image 8.

A. Experiment With the Images in the Daxinganling Area

The improved snow identification method was implemented to investigate OLI images (Images 1–3) in the Daxinganling area. Image 1 was acquired in September, and there was no snow. The pixels classified as snow account for only 0.005% of all pixels; that is, the commission error is close to 0.

Image 2 [see Fig. 6(a)] was acquired at the end of autumn, and some forest areas are covered with snow. The detected snow was overlaid with Image 2, and the result [see Fig. 6(c)] visually matches the OLI image.

In the Image 3 [see Fig. 6(b)], the forests are covered with snow, and small snow-free areas are located along roads and streets in urban areas. The snow identification result [see Fig. 6(d)] is consistent with the real scene. In total, 2.78% of total pixels in Fig. 6(d) do not contain snow, and most are distributed along roads and streets in urban areas; these pixels are accurately classified. Therefore, the omission error is far less than 2.78%.

B. Experiment With the Images in the Xiaoxinganling Area

The same method is used to evaluate the images of the Xiaoxinganling area in different seasons. There is no snow in the real scene of the Image 4, and only 0.07% of pixels are classified as snow. For images with partial snow cover, the snow identification result [see Fig. 7(c)] visually matches the Image 5 [see Fig. 7(a)]. Image 6 [see Fig. 7(b)] is almost entirely covered with snow, and the snow mapping result is shown in Fig. 7(d). The pixels recognized as no snow are mainly distributed along city roads and in the shadowed areas of the evergreen coniferous forest, and they account for 1.02% of the entire image. In this case, the omission error is less than 1.02%.

C. Experiment With the Images in the Changbai Mountain Areas

The forest in the Changbai Mountain areas is a mixed forest of broad deciduous and Korean pine trees, and Fig. 8(a) shows a typical forest scene. The OLI image (Image 7) acquired on

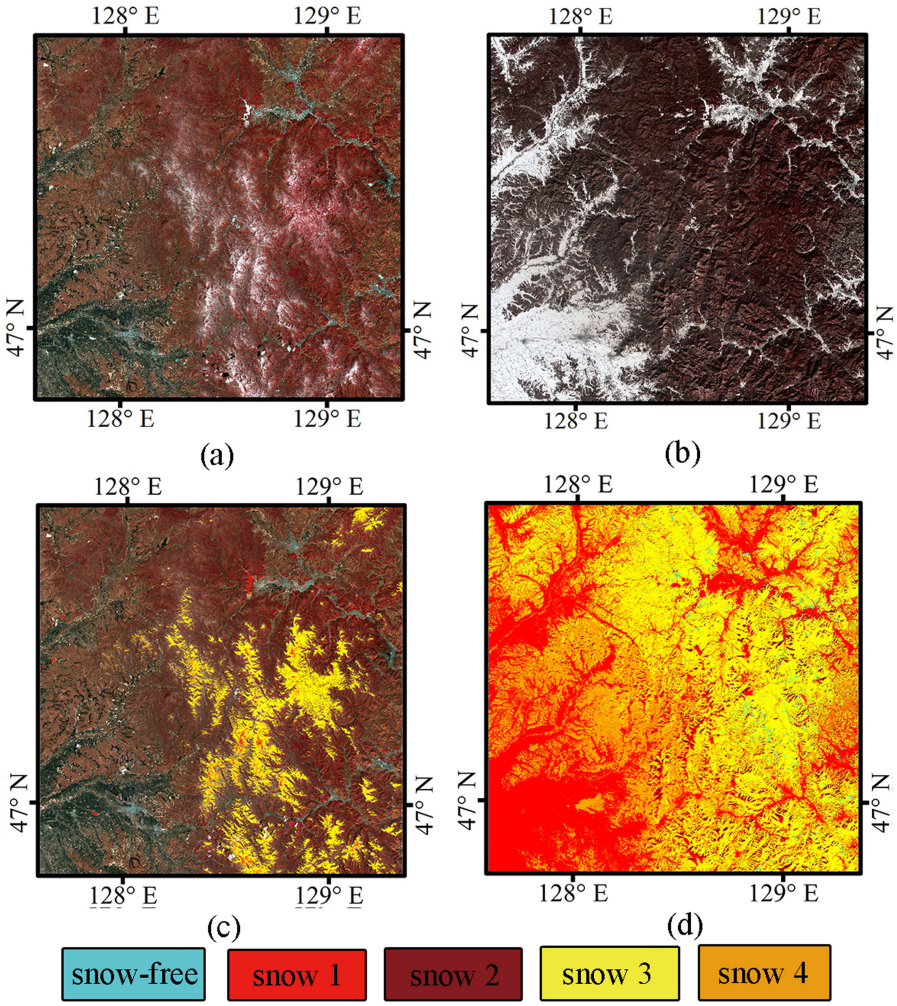

Fig. 7. OLI Images (combined with the NIR, red, and green bands) and snow identification results. (a) OLI Image 5, acquired on March 29, 2018. (b) OLI Image 6, acquired on January 24, 2018. (c) Snow identification result of the Image 5. (d) Snow identification result of the Image 6.

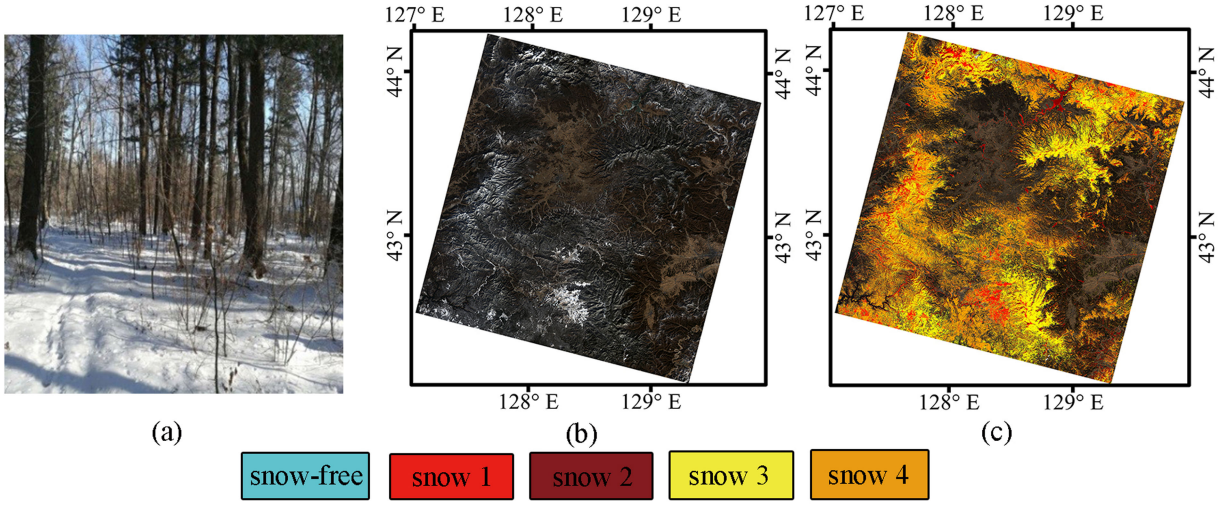

Fig. 8. (a) Typical forest scene of the Changbai Mountain areas. (b) OLI image of the Image 7. (c) Overlapping snow in the Image 7.

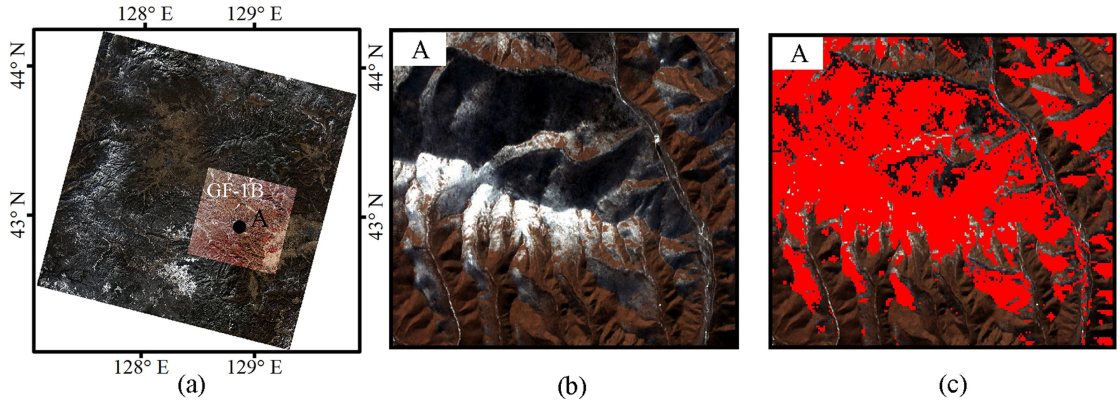

Fig. 9. (a) OLI image of the Image 7 and GF-1B PMS image. (b) Magnification of the GF-1B in the position A. (c) Binary snow identification result in the position A.

TABLE II
CONFUSION MATRIX

		Ground Truth		
		snow	snow free	total
Classification	snow	8554	97	8651
	snow free	410	11314	11724
	total	8964	11411	20375

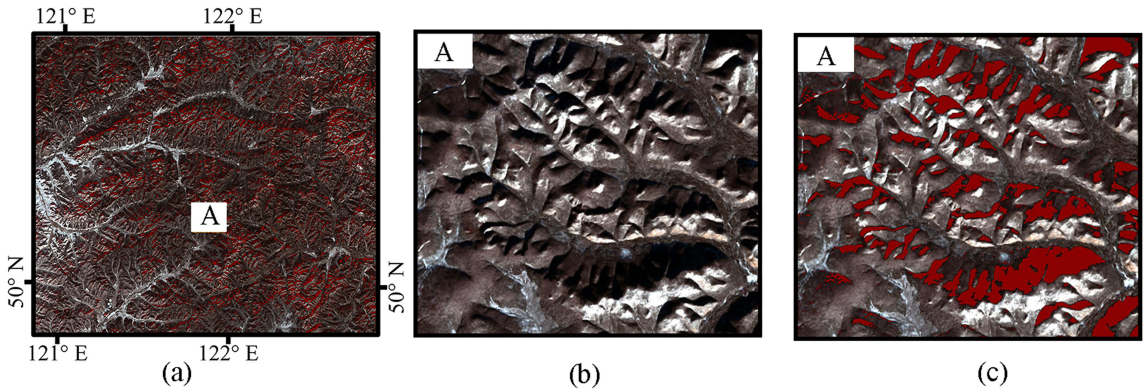

Fig. 10. (a) Overlap of snow 2 and Image 3. (b) Magnification of the OLI image of zone A. (c) Magnification of the OLI image with the snow 2 overlapping with zone A.

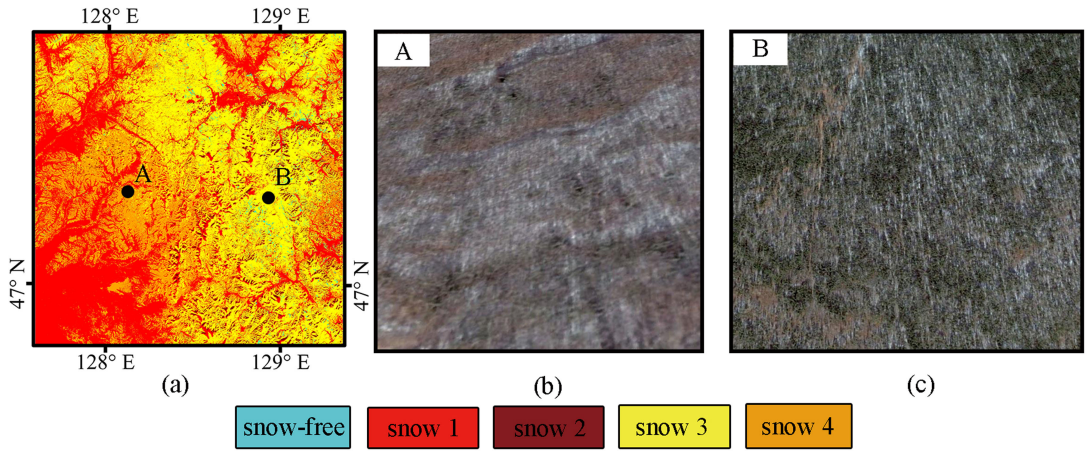

Fig. 11. (a) Snow identification result of the Image 6. Real scene at (b) point A and (c) point B.

TABLE III
REFLECTANCE INDEXES AND SNOW IDENTIFICATION RESULTS

ROI	NDSI	NDFSI	NDVI	Decision condition	Classified result
R1	0.10	0.26	0.19	NDSI<0.4 NDVI<0.25 & NDFSI>0.20	Snow 4 (snow in deciduous forest)
R2	0.31	0.53	0.40	NDSI<0.4 NDVI>0.25 & NDFSI>0.20	Snow 3 (snow in evergreen coniferous forest)
R3	0.15	0.42	0.28	NDSI<0.4 NDVI>0.25 & NDFSI>0.20	Snow 3 (snow in evergreen coniferous forest)
R4	0.03	0.28	0.23	NDSI<0.4 NDVI<0.25 & NDFSI>0.20	Snow 4 (snow in deciduous forest)
R5	-0.53	-0.12	0.26	NDSI<0	No Snow
R6	-0.04	0.43	0.56	NDSI<0	No snow
R7	-0.35	0.01	0.34	NDSI<0	No snow
R8	-0.05	0.14	0.33	NDSI<0	No snow

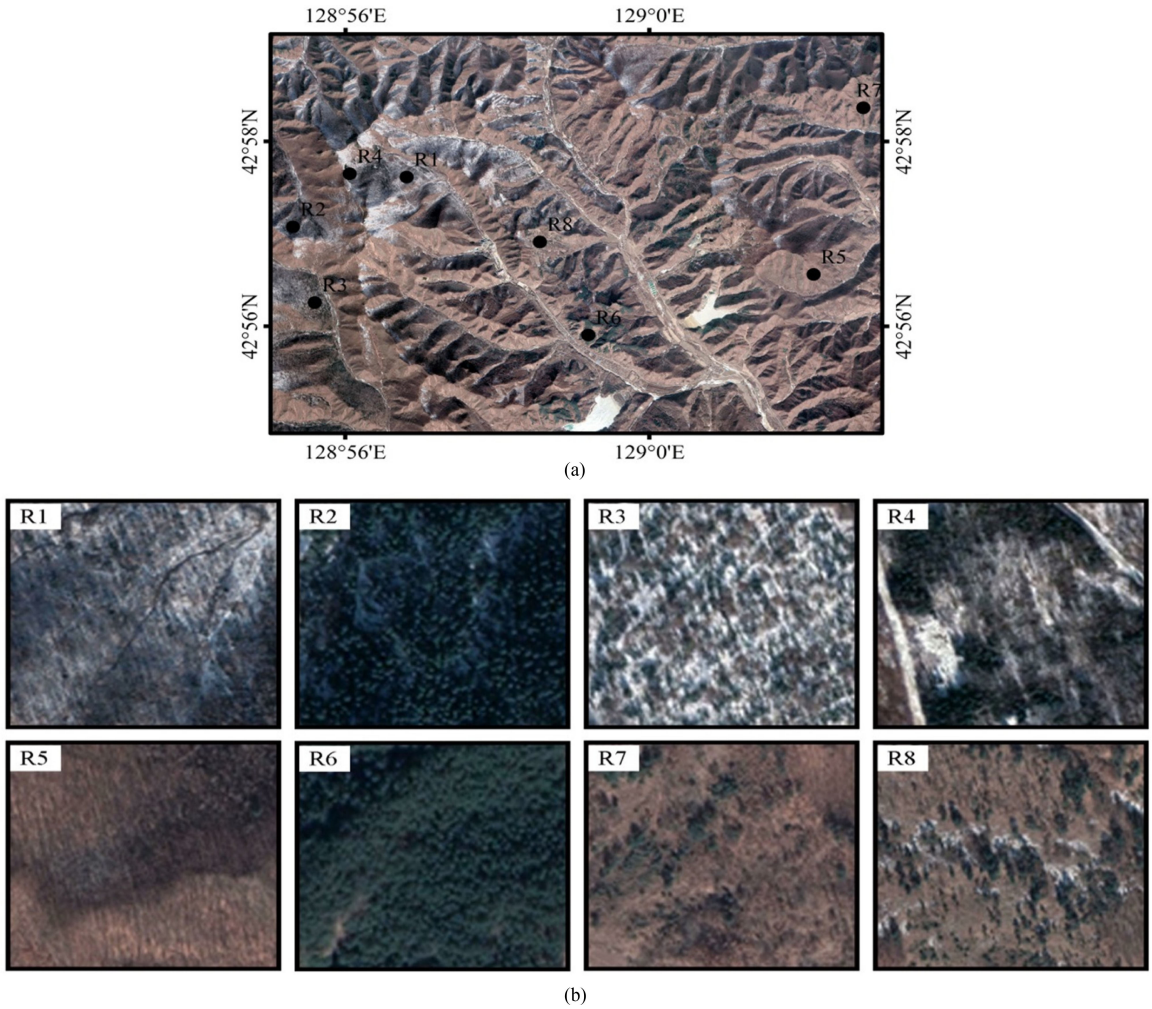

Fig. 12. (a) Google Earth Image. (b) Typical ROIs.

December 19, 2018, is shown in Fig. 8(b). Fig. 8(c) shows the overlapping detected snow and forest snow areas in the Image 7, which visually matches the OLI image. Snow in the forest areas is correctly identified, and the algorithm does not introduce commission errors in open areas. There is no obvious boundary between snow in evergreen coniferous forest (snow 3) and snow in deciduous forest (snow 4); which indicates that, the forest type is mainly mixed forest in this area.

To further verify the snow identification accuracy, a GF-1B PMS image with resolution of 2 m was chosen for quantitative assessment. Fig. 9(a) shows the GF-1B PMS image, a magnification of position A, and the binary snow identification results. In Fig. 9(b), the distribution of snow is very clear in forested areas, and Fig. 9(c) matches very well with Fig. 9(b).

Furthermore, the snow identification accuracy in forest areas is evaluated by a confusion matrix using ground-truth ROIs.

Table II shows the confusion matrix. According to Table II, the total accuracy is 97.5%, and the Kappa coefficient is 0.95. The commission and omission error of snow is 1.12% and 4.57%, respectively.

V. Discussion

A. Snow Identification in Forest Shadowed Areas

In this article, a temperature mask is added to avoid snow in shadowed forest that is mistakenly classified as liquid water. In Fig. 10(a), snow 2 overlaps to the Image 3, meaning that, the red pixels are those with NDSI$>$0.4, NIR$<$0.11, and $T<0$ °C. In the magnification, those pixels are clearly located in the shadowed forest area and snow-covered area. The statistical results show that those red pixels account for 9.2%, and the mean values of the NDSI, NIR reflectance, and land surface temperature (LST) is 0.70, 0.05, and –25 C, respectively. According to the SNOMAP without a temperature mask, those pixels will be classified as liquid water. Thus, this improvement can effectively reduce the snow omission error in shadowed forest regions at high latitudes.

B. Snow Identification in Different Forest Types

Fig. 11(a) is the snow identification results of the Image 6, which shows that snow in nonforest areas (red pixels) can be detected with the SNOMAP algorithm, and a large amount of forest snow is detected by the improved algorithm in this article. Snow in different forest types is detected with different NDFSI and NDVI threshold values. Snow 3 in the flow chart is snow in the evergreen coniferous forest, and snow 4 is snow in the deciduous forest. After using the ENVI tool "clip the view to Google Earth" to evaluate the snow identification result of the Image 6, the results are consistent with the actual scene.

To further evaluate this improved algorithm, different forest ROIs (R1–R8) are analyzed. Fig. 12 shows the Google Earth Image acquired on January 31, 2019 and the magnification of R1–R8. The distribution of snow and forest types in R1–R8 is very clear. Table III provides the corresponding reflectance indexes of R1–R8 in the OLI Image 8 and the snow identification results, and it shows that R1–R8 are all classified correctly according the improved algorithm.

In this algorithm, besides NDSI threshold, NDFSI and NDVI thresholds are needed to detect snow in different forest. However, too many thresholds increase the uncertainty of an algorithm. This algorithm is effective in Northeast China; its effectivity in other complex forest regions needs to be further tested.

VI. Conclusion

Snow cover in forest areas will be underestimated based on the SNOMAP algorithm. According to the spectrum characteristics of different forests, an improved snow identification algorithm is proposed and implemented to investigate the main forest regions in Northeast China. In addition to detecting snow in open areas with the NDSI, this algorithm combines the NDFSI and NDVI to determine whether a forest area is covered with snow. The NDFSI threshold value is different for deciduous and evergreen coniferous forests, and it can be set based on the NDVI value.

This improved method is used to analyze OLI images of the Daxinganling, Xiaoxinganling, and Changbai Mountains. In the winter images of the Daxinganling and Xiaoxinganling areas, which are fully snow covered, the omission error is less than 1%. In the autumn images without snow, the commission error is near 0. The snow identification results for the images with partial snow cover visually match the OLI images. Finally, the snow identification results for the Changbai Mountain areas are verified using a GF-1B PMS image with a 2-m spatial resolution, and the accuracy is as high as 97.5%. The Google Earth Image provides more detailed evaluation for typical ROIs, and the identification results are consistent with the real scene. The pixels that introduce errors are mainly distributed in areas of dense shadowed forest. Because of the low transmittance of the dense evergreen coniferous forest, the reflectance is very low in the corresponding shadow areas. Therefore, a small change in the reflectance can cause the reflectance indexes to fluctuate largely and introduce errors in the snow identification results. This issue is a defect of optical remote sensing. Fortunately, the proportion of these pixels is very small, and the total accuracy is still high enough for most agriculture and forest management applications.

In general, the improved snow identification method remains effective for SNOMAP in open areas and increases the classification accuracy in forest regions, regardless of whether the forest is a deciduous, evergreen coniferous, or mixed forest. Furthermore, this approach does not require a land cover map as auxiliary data; therefore, it is a simple, effective snow identification method for forest regions.

Acknowledgment

The authors like to thank the USGS for providing the experiment Landsat8 OLI images.

References

[1] J. Foster *et al.*, "Snow cover and snow mass intercomparisons of general circulation models and remotely sensed datasets," *J. Climate*, vol. 9, no. 2, pp. 409–426, Feb. 1996.

[2] G. Choi, D. Robinson, and S. Kang, "Changing northern hemisphere snow season," *J. Climate.*, vol. 23, no. 19, pp. 5305–5310, Oct. 2010.

[3] A. Hall and Q. Xin, "Using the current seasonal cycle to constrain snow albedo feedback in future climate change," *Geophys. Res. Lett.*,vol. 33, no. 3, 2006, Art. no. L03502.

[4] R. Brown and D. Robinson, "Northern Hemisphere spring snow cover variability and change over 1922–2010 including an assessment of uncertainty," *Cryosphere*, vol. 5, no. 1, pp. 219–229, 2011.

[5] A. Frei, R. A. Brown, J. A. Miller, and D.A. Robinson, "Snow mass over North America: Observations and results from the second phase of the atmospheric model intercomparison project," *J. Hydrometeorol.*, vol. 6, no. 5, pp. 681–695, 2005.

[6] A. Rango, "Spaceborne remote sensing for snow hydrology applications," *Hydrological Sci. J.*, vol. 41, no. 4, pp. 477–494, Aug. 1996.

[7] T. P. Barnett, J. C. Adam, and D. P. Lettenmaier, "Potential impacts of a warming climate on water availability in snow-dominated regions," *Nature*, vol. 438, no. 7066, pp. 303–309, 2005.

[8] R. Wu and B. P. Kirtman, "Observed relationship of spring and summer East Asian rainfall with winter and spring Eurasian snow," *J. Climate*, vol. 20, no. 7, pp. 1285–1304, 2007.

[9] R. C. Bales, N. P. Molotch, T. H. Painter, M. D. Dettinger, R. Rice, and J. Dozier, "Mountain hydrology of the western United States," *Water Resources Res.*, vol. 42, 2006, Art. no. w08432.
[10] D. Viviroli, H. H. Durr, B. Messerli, M. Meybeck, and R. Weingartner, "Mountains of the world, water towers for humanity: Typology, mapping and global significance," *Water Resources Res.*, vol. 43, 2007, Art. no. W07447.
[11] D. Viviroli, R. Weingartner, and B. Messerli, "Assessing the hydrological significance of the World's Mountains," *Mountain Res. Develop.*, vol. 23, no. 1, pp. 32–40, 2003.
[12] T. H. Painter, J. Dozier, D. A. Roberts, R. E. Davis, and R. O. Green, "Retrieval of subpixel snow-covered area and grain size from imaging spectrometer data," *Remote Sens. Environ.*, vol. 85, no. 1, pp. 64–77, 2003.
[13] T. H. Painter, K. Rittger, C. McKenzie, P. Slaughter, R.E. Davis, and J. Dozier, "Retrieval of subpixel snow covered areas, grain size, and albedo from MODIS," *Remote Sens. Environ.*, vol. 113, no. 4, pp. 868–879, 2009.
[14] J. Zhu, J. C. Shi, and Y. H. Wang, "Subpixel snow mapping of the Qinghai-Tibet plateau using MODIS data," *Int. J. Appl. Earth Observ.*, vol. 18, pp. 251–262, Aug. 2012.
[15] P. Sirgury, R. Mathieu, and Y. Arnaud, "Subpixel monitoring of the seasonal snow cover with MODIS at 250 m spatial resolution in the Southern Alps of New Zealand: Methodology and accuracy assessment," *Remote Sens. Environ.*, vol. 113, no. 1, pp. 160–181, Jan. 2009.
[16] S. Metsamaki, J. Vepsalainen, J. Pulliainen, and Y. Sucksdorff, "Improved linear interpolation method for the estimation of snow covered area from optical data," *Remote Sens. Environ.*, vol. 82, no. 1, pp. 64–78, 2002
[17] S. Metsamaki, O. P. Mattila, J. Pulliainen, K. Niemi, K. Luojus, and K. Battcher, "An optical reflectance model-based method for fractional snow cover mapping applicable to continental scale," *Remote Sens. Environ.*, vol. 123, pp. 508–521, Aug. 2012.
[18] V. V. Salomonson and I. Appel, "Development of the Aqua MODIS NDSI fractional snow cover algorithm and validation results," *IEEE Trans. Geosci. Remote Sens.*, vol. 44, no. 7, pp. 1747–1756, Jul. 2006.
[19] I. D. Dobreva and A. G. Klein, "Fractional snow cover mapping through artificial neural network analysis of MODIS surface reflectance," *Remote Sens. Environ.*, vol. 115, no. 12, pp. 3355–3366, 2011.
[20] S. Kuter, Z. Akyurek, and G. W. Weber, "Retrieval of fractional snow covered area from MODIS data by multivariate adaptive regression splines," *Remote Sens. Environ.*, vol. 205, pp. 236–252, Feb. 2018.
[21] D. K. Hall, R. Solberg, and G. A. Riggs, "Validation of satellite snow cover maps in North America and Norway," in *Proc. 59th Eastern Snow Conf.*, Stowe, VT, USA, Jun. 2002.
[22] X. W. Wang *et al.*, "Subpixel monitoring of the seasonal snow cover with MODIS at 250 m spatial resolution in the Southern Alps of New Zealand: Methodology and accuracy assessment," *Hydrol. Process.*, vol. 31, no. 18, pp. 3225–3241, Jun. 2017.
[23] H. R. Hao, L. M. Jiang, J. C. Shi, G. X. Wang, and X. J. Liu, "Assessment of MODIS-based fractional snow cover products over the Tibetan plateau," *IEEE J. Sel. Topics Appl. Earth Observ. Remote Sens.*, vol. 12, no. 2, pp. 533–548, Feb. 2019.
[24] J. Parajka, L. Holko, Z. Kostka, and G. Bloschi, "MODIS snow cover mapping accuracy in a small mountain catchment—Comparison between open and forest sites," *Hydrol. Earth Syst. Sci.*, vol. 16.no. 7, pp. 2365–2377, 2012
[25] J. Dozier, "Spectral signature of alpine snow cover from the Landsat thematic mapper," *Remote Sens. Environ.*, vol. 28, pp. 9–22, Apr. 1989.
[26] V. V. Salomonsona and I. Appelb, "Estimating fractional snow cover from MODIS using the normalized difference snow index," *Remote Sens. Environ.*, vol. 89, no. 3, pp. 351–360, 2004.
[27] D. K. Hall, G. A. Riggs, and V. V. Salomonson, "Development of methods for mapping global snow cover using moderate resolution imaging spectroradiometer data," *Remote Sens. Environ.*, vol. 54, no. 2, pp. 127–140, 1995.
[28] A. G. Klein, D. K. Hall, and G. A. Riggs, "Improving snow cover mapping in forests through the use of a canopy reflectance model," *Hydrol. Process.*, vol. 12, no. 10–11, pp. 1723–1744, Aug. 1998.
[29] D. Vikhamar and R. Solberg, "Subpixel mapping of snow cover in forests by optical remote sensing," *Remote Sens. Environ.*, vol. 84, no. 1, pp. 69–82, 2002.
[30] D. Vikhamar and R. Solberg, "Snow-cover mapping in forests by constrained linear spectral unmixing of MODIS data," *Remote Sens. Environ.*, vol. 88, no. 3, pp. 309–323, 2003.
[31] S. J. Metsämäki, S. T. Anttila, H. J. Markus, and J. M. Vepsäläinen, "A feasible method for fractional snow cover mapping in boreal zone based on a reflectance model," *Remote Sens. Environ.*, vol. 95, no. 1, pp. 77–95, Mar. 2005.
[32] E. H. Czyzowska-Wisniewski, W. J. D. van Leeuwen, K. K. Hirschboeck, S. E. Marsh, and W. T. Wisniewski, "Fractional snow cover estimation in complex alpine-forested environments using an artificial neural network," *Remote Sens. Environ.*, vol. 156, pp. 403–417, Jan. 2015.
[33] X. Y. Wang, J. Wang, Z. Y. Jiang, H. Y. Li, and X. H. Hao, "An effective method for snow-cover mapping of dense Coniferos forests in the upper Heihe river basin using Landsat operational land imager data," *Remote Sens.*, vol. 7, no. 12, pp. 17246–17257, Dec. 2015.
[34] X. Y. Wang, J. Wang, T. Che, X. D. Huang, X. H. Hao, and H. Y. Li, "Snow cover mapping for complex mountainous forested environments based on a multi-index technique," *IEEE J. Sel. Topics Appl. Earth Observ. Remote Sens.*, vol. 11, no. 5, pp. 1433–1441, May 2018.
[35] T. Che, L. Y. Dai, X. M. Zheng, X. F. Li, and K. Zhao, "Estimation of snow depth from passive microwave brightness temperature data in forest regions of northeast China," *Remote Sens. Environ.*, vol. 183, pp. 334–349, Sep. 2016.
[36] T. Sankey *et al.*, "Multi-scale analysis of snow dynamics at the southern margin of the North American continental snow distribution," *Remote Sens. Environ.*, vol. 169, pp. 307–319, Nov. 2015.
[37] C. Notarnicola *et al.*, "Snow cover maps from MODIS images at 250 m resolution, Part 2: Validation," *Remote Sens.*, vol. 5, no. 4, pp. 1568–1587, Apr. 2013.
[38] X. D. Huang, T. G. Liang, X. T. Zhang, and Z. G..Guo, "Validation of MODIS snow cover products using Landsat and ground measurements during the 2001–2005 snow seasons over northern Xinjiang, China," *Int. J. Remote Sens.*, vol. 32, no. 1, pp. 133–152, 2011.
[39] C. J. Crawford, "MODIS Terra Collection 6 fractional snow cover validation in mountainous terrain during spring snowmelt using Landsat TM and ETM+," *Hydrol. Process.*, vol. 29, pp. 128–138, 2015.
[40] X. F. Yu and D. F. Zhuang, "Monitoring forest phenophases of northeast China based on MODIS NDVI data," *Resources Sci.*, vol. 28, no. 4, pp. 111–117, 2006.

Xiaoyan Wang received the B.S. degree in optoelectronic information engineering from Shandong University, Jinan, China, in 1996, and the M.S. degree in communication and information system and the Ph.D. degree in geographic information system both from Lanzhou University, Lanzhou, China, in 2004 and 2011, respectively.

She is currently an Associate Professor with Lanzhou University. Her research interests include remote sensing image processing and remote sensing of snow.

Siyong Chen received the B.S. degree in geology from Chang'an University, Xi'an, China, in 2016. He is currently working toward the M.S. degree in cartography and geographic information systems with Lanzhou University, Lanzhou, China.

His research interests include remote sensing data reconstruction and snow parameters retrieval.

Jian Wang received the B.S. degree in autocartography from Nanjing University, Nanjing, China, in 1983, the M.S. degree in physical geography and the Ph.D. degree in geographical information systems both from the Cold and Arid Regions Environmental and Engineering Research Institute, Chinese Academy of Sciences, Lanzhou, China, in 1989 and 2004, respectively.

He is a Professor of remote sensing and GIS with the Northwest Institute of Eco-Environment and Resources, Chinese Academy of Sciences, where he is the Deputy Director with the Laboratory of Remote Sensing and Geospatial Science, and the Deputy Director with World Data Center for Glaciology and Geocryology. His research interest includes snow observations by radar and optical remote sensing data, snow hydrology, and ecosystem modeling.